AGU PUBLICATIONS

Geochemistry, Geophysics, Geosystems

RESEARCH ARTICLE
10.1002/2014GC005297

Local and regional trends in Plio-Pleistocene $\delta^{18}O$ records from benthic foraminifera

David B. Bell[1], Simon J. A. Jung[1], Dick Kroon[1], Lucas J. Lourens[2], and David A. Hodell[3]

[1]School of Geosciences, University of Edinburgh, Edinburgh, UK, [2]Faculty of Geosciences, Utrecht University, Utrecht, Netherlands, [3]Department of Earth Science, University of Cambridge, Cambridge, UK

Key Points:
- We present two new Pliocene-Pleistocene benthic stable oxygen isotope records
- Large intra-Atlantic oxygen isotope gradients are documented
- We infer new NADW component with a low-latitude surface water signal

Supporting Information:
- Readme
- Figures S1 and S2
- Text 01

Correspondence to:
D. B. Bell,
Dave.Bell@ed.ac.uk

Citation:
Bell, D. B., S. J. A. Jung, D. Kroon, L. J. Lourens, and D. A. Hodell (2014), Local and regional trends in Plio-Pleistocene $\delta^{18}O$ records from benthic foraminifera, *Geochem. Geophys. Geosyst.*, *15*, 3304–3321, doi:10.1002/2014GC005297.

Received 11 FEB 2014
Accepted 10 JUL 2014
Accepted article online 14 JUL 2014
Published online 20 AUG 2014

Abstract We present new orbital-resolution Pliocene-Pleistocene benthic stable oxygen isotope ($\delta^{18}O_b$) records from Ocean Drilling Program Sites 1264 and 1267, from Walvis Ridge in the Southeast Atlantic. We compare long-term (>250 kyr) interbasin $\delta^{18}O_b$-gradients between Pacific and North Atlantic regional stacks, as well as intra and interbasin gradients from the perspective of Walvis Ridge. The $\delta^{18}O_b$ values from Sites 1264 and 1267 are almost always higher than deep North Atlantic and Pacific sites, with large gradients (>0.5‰) emerging abruptly at ~2.4 Ma and persisting until ~1.3 Ma. From this, we infer the presence of a new water mass, which resulted from the influence of dense, ^{18}O-enriched Nordic sea overflow waters via the abyssal East Atlantic. Meanwhile, long-term average $\delta^{18}O_b$ values in the North Atlantic appear to have remained within 0–0.25‰ lower than in the Pacific. However, the magnitude of this difference is sensitive to the inclusion of records from the equatorial West Atlantic. These results, together with constraints based on temperature, salinity, and density, suggest an influence of the seawater $\delta^{18}O$ ($\delta^{18}O_{SW}$) versus salinity relationship of source waters on $\delta^{18}O_b$ values within the Atlantic. In particular, the abrupt emergence at ~2.4 Ma of higher $\delta^{18}O_b$ values at Sites 1264 and 1267, relative to North Atlantic records, appears to require a low-latitude surface water $\delta^{18}O_{SW}$ signal. This implies a connection between northward heat transport and deep water export into the abyssal East Atlantic. Hence, our results have implications for the interpretation of $\delta^{18}O_b$ records and highlight the potential for $\delta^{18}O_b$ to constrain deep Atlantic water mass sources and pathways during the Plio-Pleistocene.

1. Introduction

Stable oxygen isotope ratios measured on benthic foraminifera ($\delta^{18}O_b$) are an invaluable tool for characterizing and understanding the climate system. Long-term $\delta^{18}O_b$ records reflect changes in the temperature and $\delta^{18}O$ of ambient seawater ($\delta^{18}O_{SW}$) [*Emiliani*, 1955], the latter of which varies with the amount of ice stored on the continents [*Shackleton*, 1967] as well as changes in surface ocean circulation and the hydrological cycle in source regions [*Rohling and Bigg*, 1998; *Waelbroeck et al.*, 2002]. The $\delta^{18}O_b$ signal can be considered in terms of global and local/regional components. The global component is composed of changes in $\delta^{18}O_{SW}$ due to fluctuations in continental ice volume, which is assumed to affect all $\delta^{18}O_b$ records equally on $>10^3$ year timescales, and changes in average global deep water temperature. Meanwhile, water mass changes in $\delta^{18}O_{SW}$ and temperature that deviate from the global average constitute the local/regional component.

The ice volume contribution to the full late Pleistocene glacial-interglacial amplitude of $\delta^{18}O_b$ change, which averages around ~1.65‰ [*Lisiecki and Raymo*, 2005], has been estimated to be 1.0 ± 0.2‰ through indirect methods [*Schrag et al.*, 1996; *Shackleton*, 2000; *Adkins et al.*, 2002; *Duplessy et al.*, 2002; *Waelbroeck et al.*, 2002]. The implication is that globally averaged deep water temperature change contributes a substantial portion (~40%) to the late Pleistocene $\delta^{18}O$ signal, equating to ~2–3°C. Moreover, inverse modeling studies have revealed that the long-term ($>10^5$ year) contributions of ice volume and average deep-sea temperature on the total $\delta^{18}O_b$ signal have varied throughout the Plio-Pleistocene, with increasing contributions from temperature change back toward the Pliocene [*Bintanja and van de Wal*, 2008; *Siddall et al.*, 2010; *de Boer et al.*, 2012]. These findings are in line with insights from coupled measurements of $\delta^{18}O_b$ and deep water temperature, based on benthic foraminiferal Mg/Ca ratio paleothermometry [*Martin et al.*, 2002; *Sosdian and Rosenthal*, 2009; *Elderfield et al.*, 2012].

Local/regional changes in deep water temperature and $\delta^{18}O_{SW}$ have also been shown to be important for understanding $\delta^{18}O_b$ records during the late Pleistocene, most notably on ~10^3 year timescales during

deglaciations, during which the normal stratigraphic assumption of synchronous $\delta^{18}O_b$ change breaks down [*Skinner and Shackleton*, 2005; *Lisiecki and Raymo*, 2009; *Waelbroeck et al*., 2011]. On $>10^3$ year timescales, glacial-interglacial change in North Atlantic saw up to an additional 2°C and 0.3‰ in temperature and $\delta^{18}O_{SW}$, respectively, compared to the Pacific [*Waelbroeck et al*., 2002; *Cutler et al*., 2003]. *Zahn and Mix* [1991] showed that during the Last Glacial Maximum (LGM), $\delta^{18}O_b$ records from the deep North Atlantic (2000–4000 m) were 0.2‰ higher than those from the abyssal Atlantic (>4000 m) and the deep Pacific (2000–4000 m), possibly indicating a regional offset to the general $\delta^{18}O_b$:salinity relationship in the North Atlantic. Indeed, local/regional differences in $\delta^{18}O_b$ between the LGM and Holocene have been used to infer circulation changes and processes of deep water formation [*Bauch and Bauch*, 2001; *Meland et al*., 2008]. In addition, the benthic foraminiferal Mg/Ca-based deep-sea temperature reconstruction from Ocean Drilling Program (ODP) Site 1123 in the Southwest Pacific shows no evidence of a gradual cooling across the Mid-Pleistocene Transition (MPT) [*Elderfield et al*., 2012], whereas sediments from Deep Sea Drilling Program (DSDP) Site 607 in the North Atlantic do record a cooling of >1°C [*Sosdian and Rosenthal*, 2009]. These differences likely reflect regional temperature changes but may also result from carbonate saturation effects on epibenthic foraminifera, as used at Site 607 [*Sosdian and Rosenthal*, 2010; *Yu and Broecker*, 2010].

Only a limited number of studies have identified long-term local/regional differences in $\delta^{18}O_b$. The heaviest $\delta^{18}O_b$ values in the North Atlantic during the past ~2 million years (hereafter Myr) are recorded at ODP Site 983, in the Gardar Drift, and have been interpreted as reflecting the presence of dense overflow waters from the Nordic seas [*McIntyre et al*., 1999; *Raymo et al*., 2004]. In the early Pliocene, between ~4.7 and 3.2 million years ago (hereafter Ma), there was a reversal in the vertical $\delta^{18}O_b$ gradient between deep (ODP Site 925) and bottom (ODP Site 929) waters in the western equatorial Atlantic. *Billups et al*. [1998] interpret this observation as a temperature and salinity increase at ~3000 m depth (Site 925), possibly due to enhanced Meridional Overturning Circulation in response to the closure of the Central American Seaway. *Tian et al*. [2002] compared $\delta^{18}O_b$ records between ODP Sites 1143 and 849 in the Pacific and DSDP Site 659 in the Atlantic, suggesting a link between Northern Hemisphere ice volume growth and deep Atlantic warming during the Plio-Pleistocene.

Thus, local/regional influences on $\delta^{18}O_b$ are important for understanding $\delta^{18}O_b$ records as they affect interpretations of ice volume change and may be used to infer changes in deep water circulation and/or high-latitude conditions where deep waters form. However, long-term ($>10^5$ year) local/regional influences on $\delta^{18}O_b$ records during the Plio-Pleistocene are not well known.

Here we present two new orbital-scale resolution Plio-Pleistocene $\delta^{18}O_b$ records from ODP Sites 1264 and 1267, situated on Walvis Ridge in the Southeast Atlantic. This region represents a major export pathway for North Atlantic Deep Water (NADW) [*Arhan et al*., 2003] and has previously shown to be important for understanding past circulation changes [*Sarnthein et al*., 1994; *Bickert and Mackensen*, 2003]. In order to investigate the evolution of local and regional $\delta^{18}O_b$-gradients within the past ~5.3 Myr, we construct and compare regional averages from the North Atlantic and Pacific and assess intra and interbasin $\delta^{18}O$-gradients from the perspective of Sites 1264 and 1267.

2. Site Locations

ODP Leg 208 drilled Sites 1264 and 1267 as part of a depth transect along the more shallow sloping northern flank of Walvis Ridge [*Zachos et al*., 2004], which forms a prominent topographic feature within the Southeast Atlantic, separating the Angola Basin to the north and the Cape Basin to the south. The deep water hydrography, summarized in Figure 1, involves the mixing of NADW, Antarctic Bottom Water (AABW) and upper Circumpolar Deep Water (uCDW), and is strongly controlled by ocean bathymetry.

Walvis Ridge forms an almost impassible barrier in most locations below ~3500 m and restricts water flow up to depths of ~2500 m. However, two passages below ~4000 m exist in the southern part of the ridge near 36°S–7°W (the Walvis Passage) and 32°40′S–2°20′W [*Connary and Ewing*, 1974]. To the northeast, the ridge shallows and only two locations allow the passage of water below ~3000 m, between 28–30°S and at 22°S (the Namib Col) [*Arhan et al*., 2003]. North of Walvis Ridge, the enclosed bathymetry means that AABW influence in the Angola Basin is limited to transport through the Romanche Fracture Zone (RFZ) near the equator, with some bottom water passage permitted through the southern part of the ridge [*Connary and Ewing*, 1974]. This means that NADW dominates all depths in the Angola Basin below ~1500 m, although

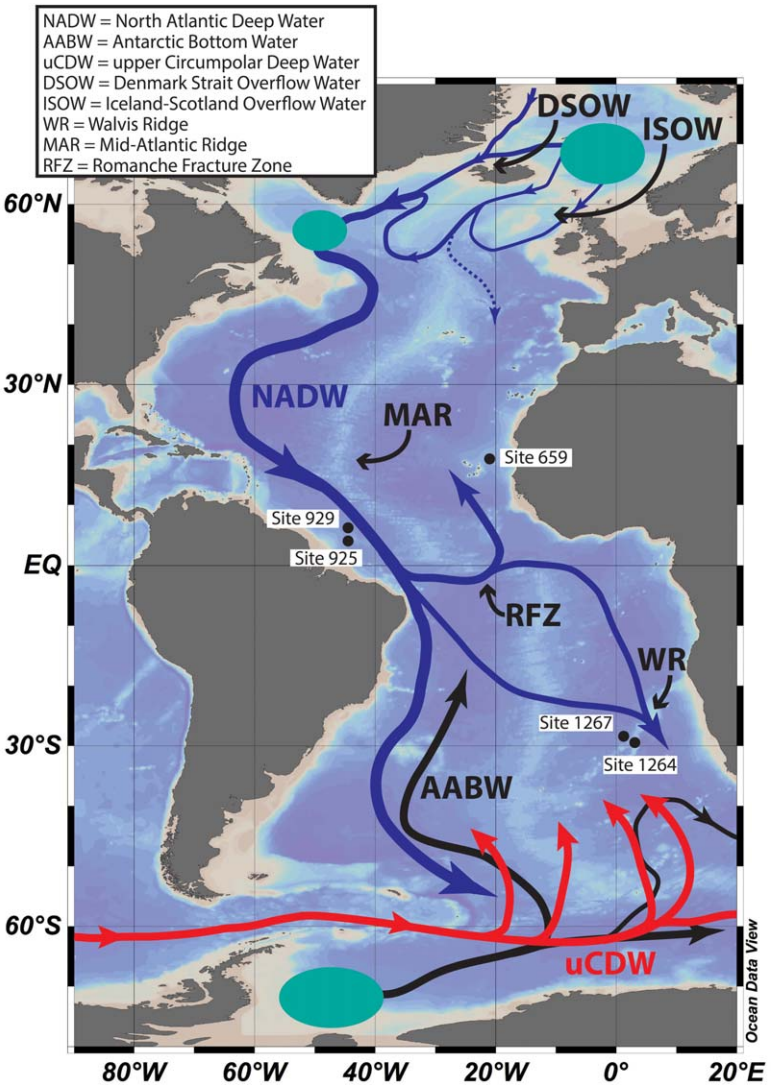

Figure 1. Schematic of Atlantic deep water (>1500 m depth) circulation with labels for key sites discussed in the text. Circulation scheme is adapted from *Dickson and Brown* [1994], *Stramma and England* [1999], and *Arhan et al.* [2003].

there is modification of the lowest parts of NADW by AABW, possibly as much as 20–30% [*Schmiedl et al.*, 1997; *Arhan et al.*, 2003]. Below the constraining depths of these ridges, NADW advection mainly occurs through the Romanche Fracture Zone (RFZ) and partly from dense overflow waters from the Nordic seas, which spill into the East Atlantic over the Greenland-Scotland Ridge (GSR) [*Smethie et al.*, 2000; *Fleischmann et al.*, 2001; *Arhan et al.*, 2003]. Above these depths, transport of NADW into the Southeast Atlantic is primarily accomplished via zonal pathways between the equator and ~25°S [*Arhan et al.*, 2003; *Hogg and Thurnherr*, 2005].

3. Methods

3.1. Stable Isotope Analysis

Sample processing and measurements for sediment cores from Sites 1264 and 1267 were carried out between three different universities and using four different mass spectrometers. For the large majority of samples, benthic species, *Cibicidoides wuellerstorfi*, were picked from the >200 μm size fraction. Stable oxygen and carbon (δ^{13}C) isotope measurements were performed on one to three specimens, depending on availability. Foraminiferal calcite was then reacted in 70–75°C orthophosphoric acid using the following carbonate preparation devices and the resulting CO_2 was then analyzed on the following mass spectrometers. At Vrije Universiteit, Amsterdam, using (1) a Finnigan 251 Gas Source mass spectrometer equipped with Kiel type automated carbonate extraction line and (2) a Themo Finnigan Delta+ mass spectrometer equipped with a Finnigan GasBench 2 preparation device. At the University of Edinburgh, a Thermo Electron Delta+ Advantage mass spectrometer was used with a Kiel carbonate III automated extraction line.

For samples between ~30 and 58 m composite depth (mcd) at Site 1264, processing was completed at the University of Florida. These samples were initially prepared as above, before picking *C. wuellerstorfi* from the >150 μm size fraction. Benthic foraminiferal tests were then cleaned in an ultrasonic bath to remove fine-grained particles and soaked in 15% H_2O_2 to remove surface organic contaminants prior to analysis. This cleaning procedure is unlikely to have a significant effect on stable isotope measurements [*Feldmeijer et al.*, 2013]. The number of specimens of *C. wuellerstorfi* varied from 1 to 4 and foraminiferal tests were crushed

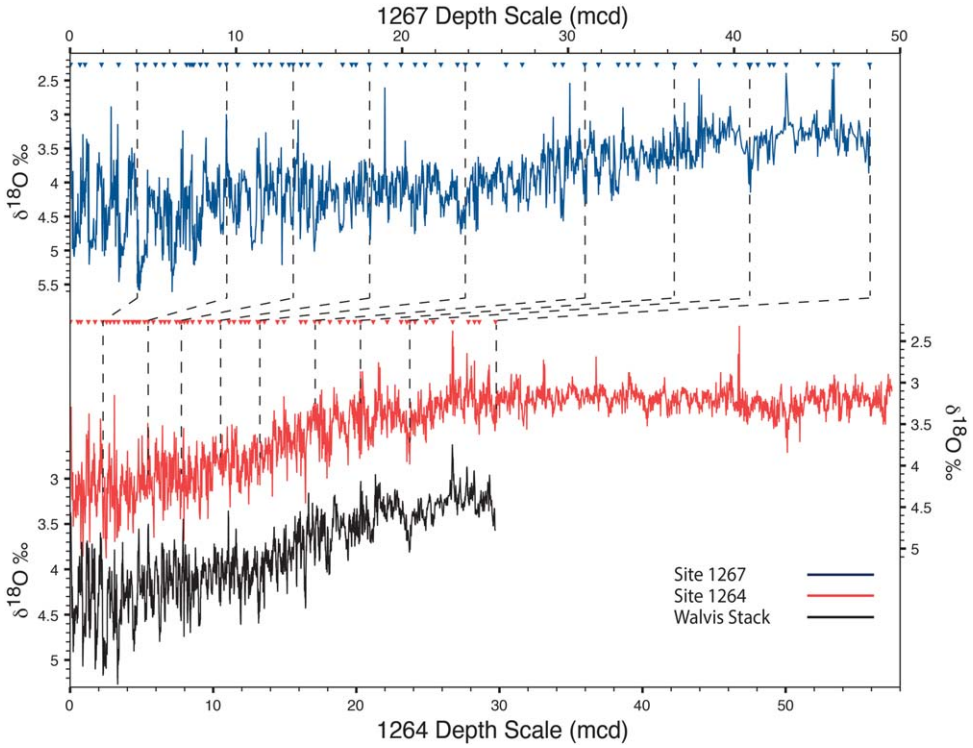

Figure 2. Visual alignment of down-core δ^{18}O data from ODP Site 1267 (top/blue) to ODP Site 1264 (middle/red) and the resulting Walvis Stack (bottom/black). The stack was created by combining data from Sites 1267 and 1264 on the 1264 depth meters composite depth (mcd) scale and smoothing by a 3pt running average. Triangular markers denote tie points used for alignment, linked by dashed lines for a select few. *C. wuellerstorfi* values are corrected by the standard +0.64% to account for disequilibrium with the surrounding seawater [*Shackleton and Hall*, 1984].

before analysis. The foraminiferal calcite was reacted in 70°C orthophosphoric acid using a Kiel III carbonate preparation device. Evolved CO_2 gas was measured online with a Finnigan-MAT 252 mass spectrometer.

For a small number of samples in Site 1267 cores, *C. wuellerstorfi* specimens were extremely sparse. A particularly sparse section was present between ~36 and 38 mcd. In the majority of these cases, alternative species, *Cibicidoides kullenbergi*, was used. For 16 measurements, *Melonis barleeanum* was used, with species-specific corrections taken from *Shackleton and Hall* [1984].

All stable isotope results are reported relative to Vienna Pee Dee Belemnite and calibrated using inhouse standards that are correlated to the international standard, NBS19. Analytical precision for both δ^{18}O and δ^{13}C for all mass spectrometers was better than $\pm 0.1‰$. *C. wuellerstorfi* δ^{18}O values are corrected for disequilibrium with surrounding seawater by $+0.64‰$ [*Shackleton and Opdyke*, 1973; *Shackleton and Hall*, 1984].

3.2. Establishment of an Orbital-Scale Age Model

For all time series processing, the software package AnalySeries was used [*Paillard et al*., 1996]. In a first step, the mcd scale of Site 1267 was mapped onto that of Site 1264, primarily via alignment of the $\delta^{18}O_b$ records (Figure 2). Whenever possible, lightness and magnetic susceptibility records were also used to improve confidence in the alignment. Once the records were aligned, data were combined to form a single continuous record, based on the Site 1264 depth scale, down to 29.7 mcd, and then averaged by a three point running mean (Figure 2). The sole purpose of this Walvis Stack is to enhance identification of $\delta^{18}O_b$ stratigraphic features, particularly with respect to Site 1264 data, which has relatively low-amplitude and low-resolution sections in the mid to late-Pleistocene.

Ideally, records of multiple parameters, independent of $\delta^{18}O_b$, would be used to establish chronology. However, in the absence of alternative records (i.e., physical or chemical measurements displaying clear orbital-scale cyclicity) from Sites 1264 and 1267, the combined $\delta^{18}O_b$ time series of the Walvis Stack and Site 1264 were visually aligned to the global $\delta^{18}O_b$ stack of *Lisiecki and Raymo* [2005] (hereafter the LR04 stack). To

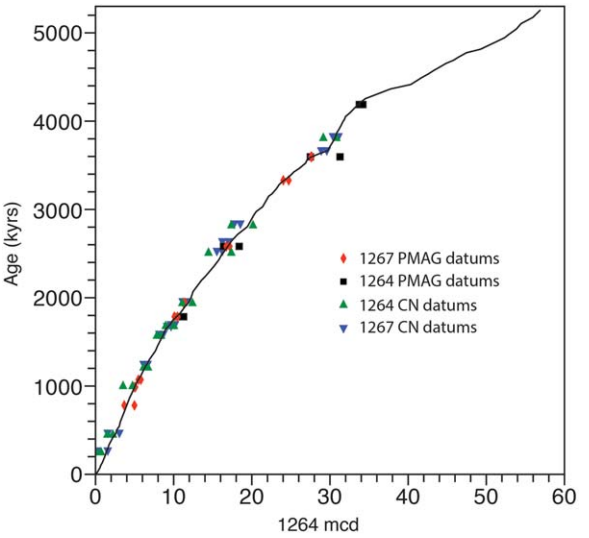

Figure 3. Walvis Ridge age model. The black line shows the age-depth relationship according to the meters composite depth scale of Site 1264. Age data from shipboard paleomagnetic reversals (PMAG) and calcareous nannofossil (CN) results show very good general agreement with the oxygen isotope derived age model.

aid in the alignment procedure and maintain consistency with independent age estimates, calcareous nannofossil (CN) and paleomagnetic reversal (PMAG) age-depth control points [*Zachos et al*., 2004] were used as initial tie points (Figure 3). Primary age control, however, was achieved through $\delta^{18}O_b$ stratigraphic alignment to the LR04 stack. The resulting age model is in agreement with all PMAG data from both Sites 1267 and 1264, with the exception of one PMAG datum, C2n (oldest date), at 1.942 Ma. Comparisons with the $\delta^{18}O_b$ stratigraphy of the LR04 stack showed sufficiently convincing similarities to justify favoring the $\delta^{18}O_b$ alignment, despite the PMAG discrepancy of ~40 kyr (supporting information Figure 1). This potential alignment error is too small to affect interpretations presented in this study. Furthermore, cross-spectral analysis demonstrates overall successful alignment of records to the LR04 stack (supporting information Figure 2). There is good general agreement with CN data, with the limited discrepancies justified by otherwise clearly poor correlation of $\delta^{18}O_b$-stratigraphy or disagreement with PMAG data, or both. Records from both Sites 1264 and 1267 are plotted on the LR04 aligned age model in Figure 4.

A notable feature of the age model for both sites is a peak in sedimentation rates around 3.6 Ma (Figure 4b). This is concurrent with marked changes in the climate system, such as an increase in Southern Ocean deep

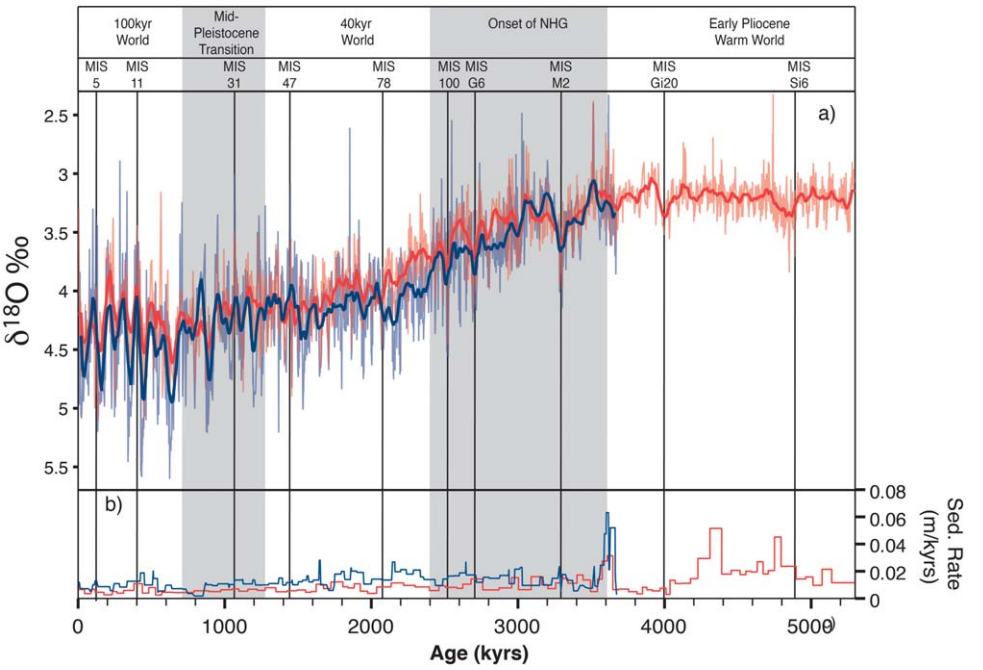

Figure 4. Walvis Ridge data versus age. (a) $\delta^{18}O$ records for Sites 1267 (blue) and 1264 (red) plotted using the LR04 aligned age model described in the main text. Thin lines are original resolution data while thick lines are smoothed using 50 kyr moving window. (b) LR04 aligned age model sedimentation rates for Sites 1267 (blue) and 1264 (red). Vertical black lines indicate prominent Marine Isotope Stages.

Table 1. Site Locations, Water Depth, Time Interval, and Sources of Isotopic Data Used in This Study

Site	Location	Water Depth (m)	Interval (Ma)	References
980	55°N, 15°W	2170	0–1	*Oppo et al.* [1998], *McManus* [1999], and *Flower et al.* [2000]
981	55°N, 15°W	2170	1–4.6	*McIntyre et al.* [1999] and *Raymo et al.* [2004]
610	53°N, 19°W	2420	2.1–3.6	*Raymo et al.* [1992]
607	41°N, 33°W	3430	0–5.3	*Raymo et al.* [1989, 1992], *Ruddiman et al.* [1989], and *Lisiecki and Raymo* [2005]
659	18°N, 21°W	3070	0–5	*Tiedemann et al.* [1994]
929	6°N, 44°W	4370	0–5.1	*Bickert et al.* [1997], *Billups et al.* [1997], and *Tiedemann and Franz* [1997]
927	5°N, 44°W	3330	0–4.2 & 4.6–5	*Bickert et al.* [1997] and *Tiedemann and Franz* [1997]
925	4°N, 43°W	3040	0–5.1	*Bickert et al.* [1997], *Billups et al.* [1997], and *Tiedemann and Franz* [1997]
664	0°N, 23°W	3800	0–1.25	*Raymo* [1997]
662	1°S, 12°W	3820	2.3–3.55	*Lisiecki and Raymo* [2005]
1020	41°N, 126°W	3040	0–1.7	*Herbert* [2001] and *Lisiecki and Raymo* [2005]
1208	36°N, 159°E	3350	1.8–3.7	*Venti and Billups* [2012]
1146	19°N, 116°E	2090	0–5	*Lisiecki and Raymo* [2005]
1143	9°N, 113°E	2770	0–5	*Tian et al.* [2002]
1241	6°N, 86°W	2030	2.5–5.3	*Tiedemann et al.* [2007]
846	3°N, 91°W	3300	0–5.3	*Mix et al.* [1995b] and *Shackleton et al.* [1995]
677	1°N, 84°W	3460	0–2.6	*Shackleton et al.* [1990]
849	0°N, 110°W	3840	0–5	*Mix et al.* [1995a]
1237	16°S, 73°W	3210	4.2–5.3	*Tiedemann et al.* [2007]
1123	42°S, 171°E	3290	0–3	*Hall et al.* [2001] and *Harris* [2002]

water ventilation [*Andersson et al.*, 2002] and the start of Northern Hemisphere ice volume increase [*Mudelsee and Raymo*, 2005; *Meyers and Hinnov*, 2010]. Hence, this transient increase in sedimentation rate possibly represents a depositional, erosional, and/or productivity response to the initiation of Northern Hemisphere glaciation.

3.3. Data Selection and Processing

In order to compare local and regional deep water $\delta^{18}O_b$ change during the Plio-Pleistocene, all available long-term (>1 Myr) $\delta^{18}O_b$ records from sites below 2000 m depth in the North Atlantic and Pacific were selected to calculate regional averages (Table 1). The use of records over 1 Myr long maintains a degree of consistency in the number and locations of cores across intervals comparable to the timescales at which we interpret the data (>250 kyr). This is to avoid, as much as possible, artifacts in the evolution of $\delta^{18}O_b$ that result from shifts in the sampling of the oceans, while maximizing the spatial coverage. We choose only records from below 2000 m for simplicity. Intermediate water masses (>2000 m), at present, often have different $\delta^{18}O_{SW}$:salinity relationships than deep waters [*LeGrande and Schmidt*, 2006; *Waelbroeck et al.*, 2011] and so variations in their isotope budget and contributions to deep water may add complexity. For both regions, and for the duration of the Plio-Pleistocene, the average number of records remains between 5 and 8, while the average depth remains between ~2800 and 3300 m. All $\delta^{18}O_b$ records have been corrected for species-specific disequilibrium with surrounding seawater by the standard values [*Shackleton and Opdyke*, 1973; *Shackleton and Hall*, 1984].

Preparing the data for comparison and creating regional averages requires records to be placed on a common timescale and a regular sampling interval. For this, we use the published chronologies for sites that have been aligned to the LR04 stack. For sites that have used alternative age model strategies, we adjusted the published age models by visually aligning the $\delta^{18}O_b$ records to the LR04 stack in order to maintain stratigraphic consistency between the different time series. All records were then resampled at 5 kyr intervals. Regional averages were calculated for the deep Pacific and North Atlantic by combining the resampled records within the respective regions. Gradients were calculated between the Pacific and North Atlantic from the difference between the two regional time series for each 5 kyr time step, then smoothed with a 50 point moving window to give 250 kyr trends (Figures 4b and 5). The use of 250 kyr running averages is to highlight trends over longer timescales than the dominant orbital-scale variability. Changing the degree of this smoothing does not affect the conclusions presented. Uncertainties in the average for the regional time series were estimated for each 5 kyr interval by calculating the 2σ standard error on the mean (SEM) before smoothing by a 50 point moving window.

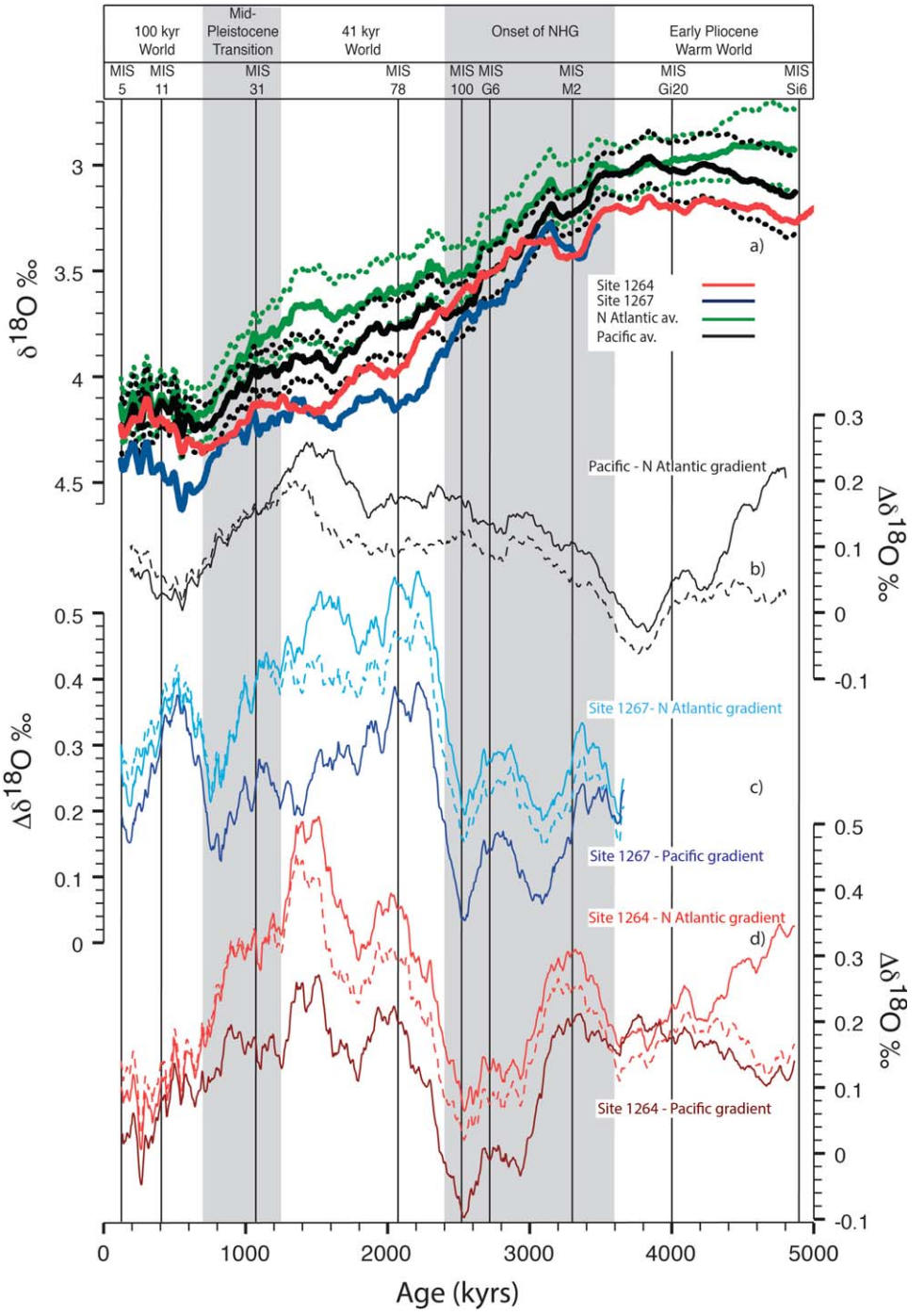

Figure 5. Long-term trends and gradients in $\delta^{18}O$. (a) 250 kyr running mean $\delta^{18}O$ values from North Atlantic and Pacific averages and Sites 1264 and 1267. Dashed lines indicate 2σ uncertainty (standard error on the mean) for the 250 kyr Pacific and North Atlantic regional averages. (b–d) 250 kyr $\delta^{18}O$-gradients as indicated on the figure. Dashed lines represent $\delta^{18}O$-gradients when Ceara Rise Sites 925, 927, and 929 are excluded from the North Atlantic average. Prominent Marine Isotope Stages are labeled, as are different transitions in the evolution of Plio-Pleistocene climate.

4. Results

During the Plio-Pleistocene, long-term (250 kyr) regional averages of the North Atlantic and Pacific show $\delta^{18}O_b$-gradients ($\delta^{18}O_{P\text{-}NA}$) varying in the range ~0–0.25‰, with the North Atlantic average consistently lower than or equal to the Pacific average (Figures 5a and 5b). $\delta^{18}O_{P\text{-}NA}$ gradients of >0.15‰ occur during

the earliest Pliocene (~5.0–4.5 Ma) and in the early to mid-Pleistocene (~2.4–1.0 Ma), while peak gradients of ~0.25‰ occur between ~1.6 and 1.4 Ma. However, these differences are largely within the range of uncertainty with regard to the mean of the records sampled (i.e., 2σ SEM), which varies between ±0.1–0.2‰ for each region (Figure 5a). Moreover, much of the $\delta^{18}O_{P\text{-}NA}$ gradient results from the inclusion of Sites 925, 927, and 929, which are located on a depth transect of Ceara Rise, in the western equatorial North Atlantic. $\delta^{18}O_{P\text{-}NA}$ gradients calculated excluding Ceara Rise sites (dashed lines in Figure 5b) are reduced throughout the Pliocene to mid-Pleistocene (~5.0–1.2 Ma), with the largest gradients (0.2‰) at ~1.4 Ma. The most prominent difference (<Δ0.2‰) between $\delta^{18}O_{P\text{-}NA}$ gradients calculated with and without Ceara Rise sites included occurs during the early Pliocene (~5.0–4.5 Ma) (Figure 5b).

The $\delta^{18}O_b$ records for Sites 1264 and 1267 are distinct from both the North Atlantic and the Pacific averages, displaying consistently higher values and a larger rate of increase during the early Pleistocene (Figures 5a, 5c, and 5d). During the earliest Pliocene (~5.0–4.5 Ma), the $\delta^{18}O_b$-gradient between Site 1264 and the North Atlantic average ($\delta^{18}O_{1264\text{-}NA}$) displays similar features to that of the $\delta^{18}O_{P\text{-}NA}$ gradient, with large differences also dependent on the inclusion of Ceara Rise sites. The most prominent $\delta^{18}O_{1264\text{-}NA}$ and $\delta^{18}O_{1267\text{-}NA}$ gradients occur during the early to mid-Pleistocene (~2.4–1.3 Ma), concurrent with maximum $\delta^{18}O_{P\text{-}NA}$ gradients. However, gradients with respect to Walvis Ridge reach more substantial maximum 250 kyr average values of ~0.5‰ (Figures 5c and 5d). If Ceara Rise sites are excluded from the North Atlantic average, then $\delta^{18}O_{1264\text{-}NA}$ and $\delta^{18}O_{1267\text{-}NA}$ gradients still reach >0.4‰ during this period (dashed lines in Figures 5c and 5d), indicating that these gradients emerge primarily as the result of the local/regional $\delta^{18}O_b$ evolution recorded at Walvis Ridge sites.

During the MPT, between ~1.25 and 0.7 Ma, $\delta^{18}O_{1264\text{-}NA}$ and $\delta^{18}O_{1267\text{-}NA}$ gradients reduce to levels similar to those observed in the Pliocene. This is in line with $\delta^{18}O_{P\text{-}NA}$ changes, reflecting a higher rater of $\delta^{18}O_b$ increase in the North Atlantic, compared to other locations. Subsequently, $\delta^{18}O_{1264\text{-}NA}$ gradients continue to reduce, while $\delta^{18}O_{1267\text{-}NA}$ gradients show a second peak, with values of ~0.35–0.4‰ between 0.35 and 0.65 Ma. The latter observation is the result of comparatively high $\delta^{18}O_b$ values at Site 1267 during Marine Isotope Stages (MISs) 10 to 16.

Long-term (250 kyr) average $\delta^{13}C$ records for Sites 1264 and 1267 are presented in Figure 6, along side data from sites in the North Atlantic, South Atlantic, and Pacific. The data show that long-term average conditions at Sites 1264 and 1267 are characterized by high $\delta^{13}C$ values, similar to values recorded in the North Atlantic and distinct from values seen south of Walvis Ridge and in the Pacific. A notable feature at Site 1264 is a maximum in $\delta^{13}C$ values between ~2.1 and 1.4 Ma, with average values increasing above those recorded at Site 925 at ~2.4 Ma. A similar increase is seen at Site 1267, although average values are lower than Site 1264, primarily due to low glacial values at Site 1267.

5. Discussion

5.1. Potential Nonclimatic Effects on $\delta^{18}O_b$ Values

There are a number of secondary effects that may influence $\delta^{18}O_b$ values, including; species-specific vital effects, seawater carbonate chemistry, and preservation effects. The records used in this study are based primarily on *C. wuellerstorfi* analysis and with appropriate species-specific corrects made when other species are used. Hence, differences in species vital effects are avoided. Seawater carbonate ion concentration, [CO_3^{2-}], meanwhile, has been shown to affect the $\delta^{18}O$ of planktonic and benthic foraminifera [*Spero et al.*, 1997; *Rathmann and Kuhnert*, 2008]. We do not consider this to be an issue, however, as [CO_3^{2-}] changes large enough to explain the observed intra-Atlantic $\delta^{18}O_b$-gradients would require concomitant $\delta^{13}C$-gradients, which are not observed (Figure 6). Finally, while care was taken to select only well-preserved *C. wuellerstorfi* specimens for the construction of stable isotope records at Sites 1264 and 1267, preservation effects were not directly addressed during this study. However, a recent study by *Edgar et al.* [2013] has shown that diagenetic alteration to benthic foraminiferal calcite has negligible impact on whole-test stable isotope values (~<0.13‰ for both $\delta^{13}C$ and $\delta^{18}O_b$).

Systematic interlaboratory offsets are an additional possible factor influencing $\delta^{18}O_b$-gradients. Indeed, our experience from a small number of duplicate measurements taken between different laboratories indicates potential offsets of up to 0.1–0.2‰. This is in line with previous findings of up to 0.3‰ [*Ostermann and Curry*, 2000]. However, given practical limitations on the number of duplicate measurements possible, including limited availability of *C. wuellerstorfi* specimens, such offsets are difficult to correct for. Hence, we are aware of potential offsets of <0.3‰. Nevertheless, we emphasize that the gradients with respect to Sites

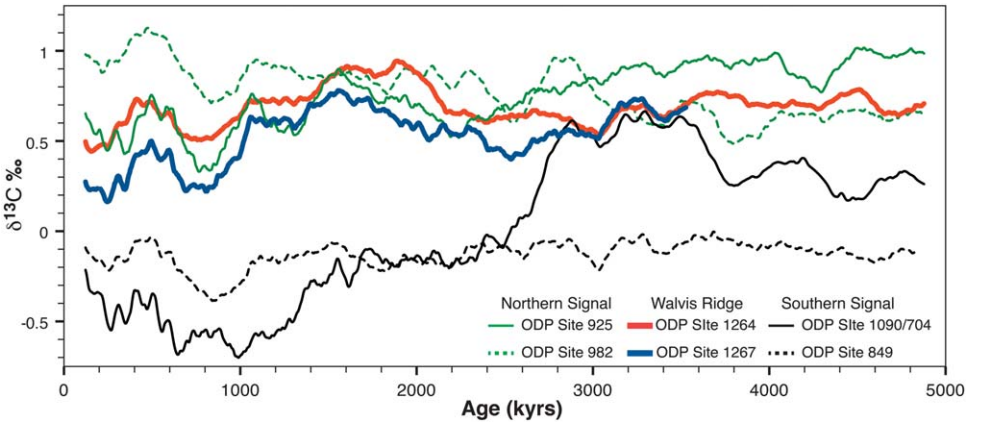

Figure 6. Long-term (250 kyr) average $\delta^{13}C$ records indicating the source region for deep waters bathing Sites 1264 and 1267. Data are from Site 982 [*Venz and Hodell*, 2002; *Hodell and Venz-curtis*, 2006], Site 925 [*Bickert et al*., 1997; *Billups et al*., 1997; *Tiedemann and Franz*, 1997], Site 704 [*Hodell and Venz*, 1992], Site 1090 [*Venz and Hodell*, 2002], and Site 849 [*Mix et al*., 1995a].

1264 and 1267 interpreted in this study are substantially larger than this uncertainty ($>0.5‰$), and the influence of offsets in regional averages should be minimal. Furthermore, the observation that both Site 1264 and 1267 $\delta^{18}O_b$ data are consistently higher than the Atlantic and Pacific averages, despite being measured across multiple laboratories, gives confidence to this finding.

5.2. Climatic Factors Affecting Local/Regional Differences in $\delta^{18}O_b$

The effect of ice volume change on $\delta^{18}O_b$ is considered synchronous on $>10^3$ year timescales and should affect all records equally. Hence, differences between $\delta^{18}O_b$ records imply local/regional changes in deep water temperature and $\delta^{18}O_{SW}$. Because deep waters (>2000 m depth) are formed through the cooling and densification of high-latitude surface waters, these changes will reflect variations in high-latitude climate, the processes and water masses involved in deep water formation and mixing between deep water masses.

On a regional basis, $\delta^{18}O_{SW}$ is correlated to salinity through common controls in the hydrological cycle, such as evaporation and precipitation [*Craig and Gordon*, 1965]. Thus, local/regional differences in $\delta^{18}O_b$ are correlated to seawater density through changes in temperature and salinity. However, this correlation is complicated by changes in the $\delta^{18}O_{SW}$:salinity relationship through time. In the case of a two end-member freshwater-seawater mixing regime, the $\delta^{18}O_{SW}$:salinity relationship for any given surface region in the ocean is determined by the ratio of the differences in end-member $\delta^{18}O$ and salinity, with the y-intercept (i.e., zero salinity value) set by the value of freshwater $\delta^{18}O$. Even in this simplified scenario, it has been demonstrated that substantial variations in regional $\delta^{18}O_{SW}$:salinity between glacial and interglacial times may occur (slope changes of a factor of $\sim$1/3 to 2, depending on the oceanic setting) merely by altering the freshwater end-member within conservative bounds [*Rohling and Bigg*, 1998]. Meanwhile, sea ice formation acts to increase salinity with little noticeable change in $\delta^{18}O_{SW}$ [*Craig and Gordon*, 1965], such as during deep water formation around Antarctica [*Weiss et al*., 1979; *Leonard et al*., 2011]. Additional complications may also arise when considering changes to the local evaporation-precipitation balance, changes in freshwater volume flux, additional freshwater end-members, and mixing between upper ocean water masses [*Rohling and Bigg*, 1998]. Factors such as these may lead to significant changes in $\delta^{18}O$-gradients recorded by foraminifera without requiring any change in the temperature, salinity, or density of the ambient seawater [*Schmidt*, 1999].

The situation for $\delta^{18}O$-gradients recorded by benthic foraminifera is expected to be less variable than for planktonic foraminifera, as minimum density requirements for deep water formation reduce the total range of salinity and temperature. However, within the North Atlantic, especially at high latitudes, local $\delta^{18}O_{SW}$:salinity variations between potential areas of deep water formation are likely larger than other regions. This is because of the large range of possible freshwater and seawater end-members, the varying locations of deep water production, and the strongly varying influence of sea ice formation through time [e.g., *Duplessy et al*., 1988; *Wadley et al*., 2002]. Additionally, deep waters originating from marginal basins, such as the

Nordic seas or the Mediterranean, are also susceptible to large changes in the local $\delta^{18}O_{SW}$:salinity relationship [*Rohling and Bigg*, 1998].

In the modern ocean, although deep waters in the North Atlantic have higher $\delta^{18}O_{SW}$ values than those in the Pacific, the higher deep water temperatures in the North Atlantic approximately offset this difference, resulting in relatively uniform $\delta^{18}O$-calcite equivalent values for a given depth [*Zahn and Mix*, 1991]. The observation of interbasin and intrabasin $\delta^{18}O_b$-gradients in the past will, therefore, indicate differences in water mass properties, processes of deep water formation, and/or deep water circulation, that are distinct from modern conditions [e.g., *Zahn and Mix*, 1991; *Billups et al*., 1998].

5.3. Local/Regional Trends in $\delta^{18}O_b$

Despite only small $\delta^{18}O_b$ differences between the Pacific and North Atlantic averages during the Plio-Pleistocene, values are always positive when gradients develop. This observation is not readily explained by artifacts resulting from changes in temperature with depth, as the average site depth for both regional averages remains between ~2800 and 3300 m. Instead, positive $\delta^{18}O_b$-gradients (e.g., at ~1.5 Ma) likely reflect times when the North Atlantic was filled with deep waters that had larger temperature differences and/or smaller $\delta^{18}O_{SW}$ differences with the Pacific, relative to the present.

The notable changes in $\delta^{18}O_{P\text{-}NA}$ gradients which are dependent on the inclusion of Ceara Rise records to the North Atlantic average, suggest that North Atlantic intrabasin variability is a significant factor in calculating regional gradients. Hence, this finding complicates interpretations of regional differences from gradients between individual records [e.g., *Tian et al*., 2002]. However, while the magnitude of the $\delta^{18}O_{P\text{-}NA}$ gradient that emerges during the early Pliocene (at ~3.6 Ma) is affected by the inclusion of Ceara Rise sites, the sign and trend remain. Thus, we suggest that average deep water $\delta^{18}O_b$ values in the North Atlantic were lower than in the Pacific during the early to mid-Pleistocene. Relatively warmer temperatures in the North Atlantic as an explanation for this difference is consistent with the sign of differences in bottom water temperature reconstructions between Pacific Site 1123 [*Elderfield et al*., 2012] and North Atlantic Site 607 [*Sosdian and Rosenthal*, 2009]. However, the pre-MPT $\delta^{18}O_{1123\text{-}607}$ gradient of ~0.29‰, which is similar to the $\delta^{18}O_{P\text{-}NA}$ gradient, can only account for approximately half the temperature difference of ~2.3°C (calculated from differences in 250 kyr averages).

The $\delta^{18}O_b$-gradient that emerges after ~2.4 Ma at Walvis Ridge sites coincides with positive $\delta^{18}O_{P\text{-}NA}$ gradients but is considerably larger and more abrupt. This indicates the emergence of a unique water mass within the Southeast Atlantic during the early to mid-Pleistocene, with higher $\delta^{18}O_b$ values than both the deep North Atlantic and deep Pacific. Comparisons between $\delta^{13}C$ records from the North Atlantic, South Atlantic, Pacific, and Walvis Ridge strongly indicate that deep waters bathing Walvis Ridge sites are predominantly northern sourced (Figure 6). Hence, in order to reconcile the observed large $\delta^{18}O$-gradients, we suggest that at least two separate sources of NADW filled the Atlantic.

Existing $\delta^{18}O_b$ records from cores located in the Atlantic provide constraints on the origin of the $\delta^{18}O_b$ signal at Walvis Ridge sites (Figure 1). Sites 925 (3040 m) and 929 (4350 m) are located at comparable depths to Sites 1264 (2505 m) and 1267 (4350 m), respectively. Site 929 is located close to the RFZ on the western side of the MAR and is at an appropriate depth to monitor deep water properties entering the Southeast Atlantic through this pathway. Along the East Atlantic to the north of Walvis Ridge sites, Site 659 (3080 m) provides constraints on water mass properties entering the Southeast Atlantic along the eastern basins, at a depth similar to Site 1264.

Figure 7 shows comparisons of $\delta^{18}O_b$ records from Walvis Ridge sites, Ceara Rise sites and Site 659 between 2.5 and 1.0 Ma, when maximum $\delta^{18}O_b$-gradients occur. $\delta^{18}O_b$-gradients between Sites 1267 and 929, which both lie at ~4350 m depth, average ~0.4–0.6‰ during this interval. Larger gradients ($\Delta\delta^{18}O_b$ = ~0.6–1.0‰) occur during interglacial (low $\delta^{18}O_b$) MISs compared to glacial (high $\delta^{18}O_b$) MISs ($\Delta\delta^{18}O$ = ~0.3–0.6‰). Similar $\delta^{18}O_b$-gradients are seen between Sites 1264 and 925, and between Sites 1264 and 659, although Sites 1264–659 gradients are lower during glacials ($\Delta\delta^{18}O_b$ = ~0–0.3‰) and on average ($\Delta\delta^{18}O_b$ = ~0.2–0.5‰). The larger gradients observed during interglacials support our interpretation of differences in water mass properties as NADW formation is expected to be more vigorous at these times [*Imbrie et al*., 1992], strengthening water mass gradients. Because $\delta^{18}O_b$ is largely a function of $\delta^{18}O_{SW}$ and temperature, and these are both conservative tracers, the large $\delta^{18}O_b$-gradients in Figure 7 are not easily reconcilable with common

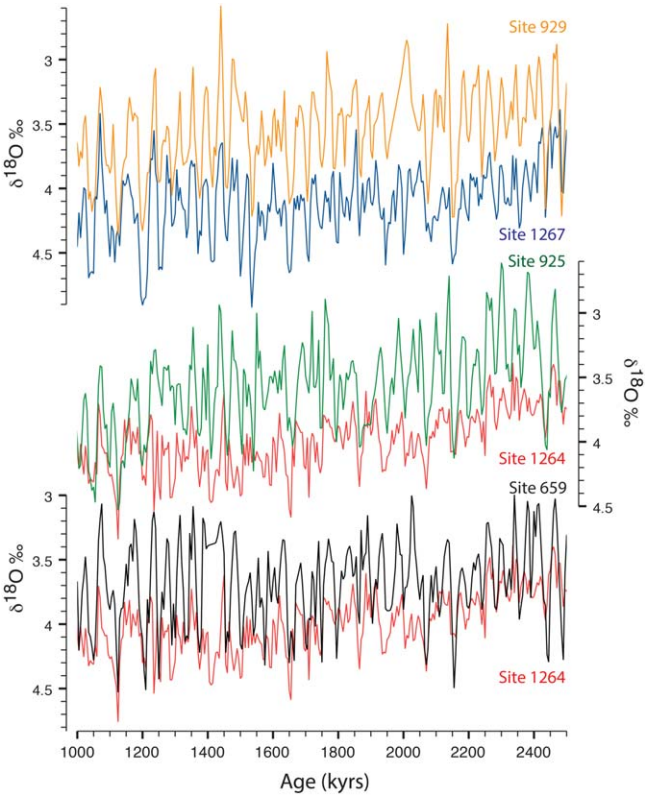

Figure 7. Comparisons of original resolution $\delta^{18}O$ time series data between Walvis Ridge Sites 1264 and 1267 and Sites in the North Atlantic encompassing the period of maximum Atlantic $\delta^{18}O$-gradients (~2.4–1.3 Ma), described in the main text.

water mass properties between the northern flank of Walvis Ridge and the locations of Sites 925, 929, and 659 (Figure 1). The RFZ and the East Atlantic at depths of ~3000 m can therefore be reasonably excluded as possible pathways for prevailing deep waters at Walvis Ridge sites.

Hence, we suggest that the abrupt emergence of $\delta^{18}O_b$-gradients at Walvis Ridge sites is due to changes in the physical properties and/or export of dense overflow waters from the Nordic seas, at ~2.4 Ma. The $\delta^{18}O_b$-gradient between Sites 1264 and 659, which occupy similar depths, may be explained if overflow waters from the Nordic seas were sufficiently dense so as to largely prevent mixing with the overlying deep waters that bathe Site 659. The topographic barrier of the Walvis Ridge would have subsequently prevented uninterrupted flow of overflow waters out of the Southeast Atlantic sector. This would have resulted in the piling up of these extradense waters, eventually also being recorded at Site 1264. This interpretation is supported by the lower development rate of $\delta^{18}O_b$-gradients at Site 1264, compared to Site 1267, at ~2.4 Ma, as there would have been a greater mixing with overlying deep waters at Site 1264 (Figures 5c and 5d). $\delta^{13}C$ records also support the interpretation of circulation changes affecting Walvis Ridge sites at ~2.4 Ma, as both sites begin a long-term increase in $\delta^{13}C$, with average values at Site 1264 becoming higher than those at Site 925 for the first time (Figure 6). Finally, these conclusions are further strengthened by previous studies that have documented similarly high $\delta^{18}O_b$ values at Site 983 in the Northeastern Atlantic since ~2.0 Ma, a site which monitors Iceland-Scotland Over Water (ISOW) [*McIntyre et al.*, 1999; *Raymo et al.*, 2004].

At present, ISOW exits the Nordic seas primarily through the Faroe Bank Channel and Wyville-Thompson Ridge, to the east of the MAR. Prior to mixing and entrainment into surrounding intermediate and deep water masses, ISOW is well stratified, with the densest components resembling source waters in the Nordic seas [*Hansen and Østerhus*, 2000]. While most of ISOW is entrained in surrounding Atlantic water masses, forming North East Atlantic Deep Water, parts continue southward in the isolated deep eastern basin [*Smethie et al.*, 2000; *Fleischmann et al.*, 2001]. If the flux of sufficiently dense waters from Nordic seas were to have increased, then it is conceivable that limited mixing with other water masses allowed the formation of a unique water mass. Despite potential similarities to the formation of ISOW, however, the situation of superdense Nordic sea overflow waters filling the abyssal East Atlantic has no modern counterpart.

An additional possible explanation for changes in deep water conditions at Walvis Ridge sites relates to changes in the flux and/or properties of Mediterranean Outflow Water (MOW). MOW exits the Mediterranean basin through the Strait of Gibraltar as a highly saline (38.4 psu), warm (13°C) and, therefore, dense water mass [*Candela*, 2001]. On entering the eastern North Atlantic and mixing with ambient North Atlantic Central Water, MOW spreads westward and northward at a depth of ~1100 m [*Lozier et al.*, 1995]. The contribution of MOW to the northeastern North Atlantic increases the salinity of intermediate waters there, thus increasing their density. In this way, MOW is considered to contribute to NADW formation [*Reid*, 1994].

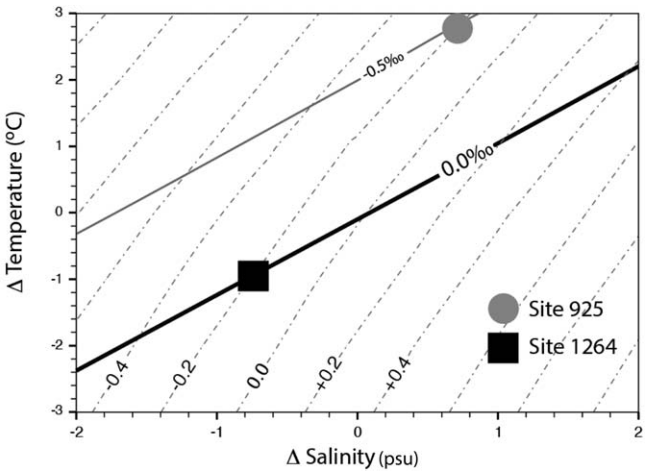

Figure 8. Assessing the implications of large (>0.5‰) Walvis Ridge-North Atlantic δ^{18}O-gradients between ~2.0 and 1.5 Ma. Temperature, salinity, and water mass density anomalies (dashed lines) are shown for the scenario in which source waters for Sites 1264 and 925 have the same regional $\delta^{18}O_{SW}$:salinity relationship. The figure shows a potential solution for the relative temperature and salinity values of Sites 1264 and 925 assuming a δ^{18}O-gradient of 0.5‰ and minimal density differences. δ^{18}O isolines (solid lines) are calculated using the paleotemperature equation from *Kim and O'Neil* [1997] and the $\delta^{18}O_{SW}$:salinity relationship $\delta^{18}O_{SW} = 0.551 \times S - 19$. Density isolines are calculated for a depth of 2770 m (σ_{2770}).

δ^{13}C reconstructions of Atlantic deep water circulation during the LGM indicate that MOW influence on deep water formation increased, while the water mass also spread southward to at least 30°S in the East Atlantic between ~1200 and 1900 m [*Zahn and Sarnthein*, 1987; *Bickert and Mackensen*, 2003]. Hence, it is possible that high $\delta^{18}O_b$ values in the Eastern Atlantic are also affected by high salinities and high $\delta^{18}O_{SW}$ values originating from MOW.

5.4. Implications of Pleistocene Atlantic $\delta^{18}O_b$-Gradients

The observation of large (>0.5‰) $\delta^{18}O_b$-gradients at times within the Atlantic poses an interesting challenge to our understanding of the controls on $\delta^{18}O_b$, more so than simply considering the scaling between temperature and $\delta^{18}O_{SW}$ contributions. This is because, at face value, $\delta^{18}O_b$-gradients of >0.5‰ would require a substantial difference in density (<~Δ0.4σ) due to differences in deep water temperature (<~Δ3.5°C) and/or salinity (<~Δ1.5 psu) (Figure 8). However, large intrabasin $\delta^{18}O_b$-gradients may be reconciled if we consider the presence of separate northern sourced water masses, with different $\delta^{18}O_{SW}$:salinity relationships. Figures 8–10 illustrate and explore this point.

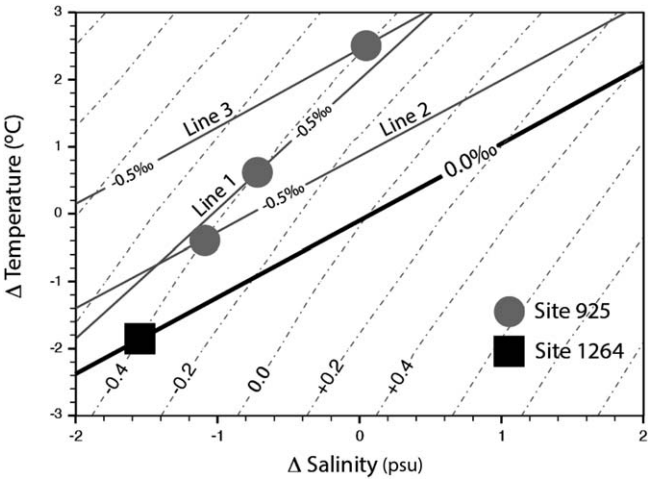

Figure 9. Assessing the implications of large (>0.5‰) Walvis Ridge-North Atlantic δ^{18}O-gradients between ~2.0 and 1.5 Ma. Temperature, salinity, and water mass density anomalies (dashed lines) are shown for scenarios in which freshwater and seawater end-members are changed to yield various $\delta^{18}O_{SW}$:salinity relationships. The figure shows a potential solutions for the relative temperature and salinity values of Sites 1264 and 925 assuming a δ^{18}O-gradient of 0.5‰ and minimal density differences for three different $\delta^{18}O_{SW}$:salinity scenarios, using the paleotemperature equation from *Kim and O'Neil* [1997]. The δ^{18}O isoline (thick black line) for Site 1264 is calculated using the $\delta^{18}O_{SW}$:salinity relationship $\delta^{18}O_{SW} = 0.551 \times S - 19$. For Line 1, the freshwater δ^{18}O value was lowered from −19‰ to −29‰, yielding a $\delta^{18}O_{SW}$:salinity relationship of $\delta^{18}O_{SW} = 0.836 \times S - 29$. For Line 2, the seawater δ^{18}O value was lowered from 0.27‰ to 0.00‰, yielding a $\delta^{18}O_{SW}$:salinity relationship of $\delta^{18}O_{seawater} = 0.543 \times S - 19$. For Line 3, the seawater salinity value was lowered from 35.0 to 34.8 psu, yielding a $\delta^{18}O_{SW}$:salinity relationship of $\delta^{18}O_{seawater} = 0.554 \times S - 19$. Density isolines are calculated for a depth of 2770 m (σ_{2770}).

Here we consider the case of Site 1264–925 δ^{18}O-gradients of 0.5‰, such as what is observed at times between ~2.0 and 1.5 Ma (Figure 7), when the presence of high δ^{13}C values indicate a northern source for deep waters at both sites (Figure 6). Figures 8–10 show a range of possible temperature, salinity, and density differences between Sites 1264 and 925, for a $\delta^{18}O_b$-gradient of 0.5‰, under different scenarios of source water $\delta^{18}O_{SW}$:salinity changes. Lines of equal density (isopycnals) are calculated from temperature and salinity values at 0.2σ intervals, assuming a depth of 2770 m (i.e., midway between Sites 1264 (2505 m) and 925 (3040 m)). Isolines of (equal) $\delta^{18}O_b$ values were calculated from the

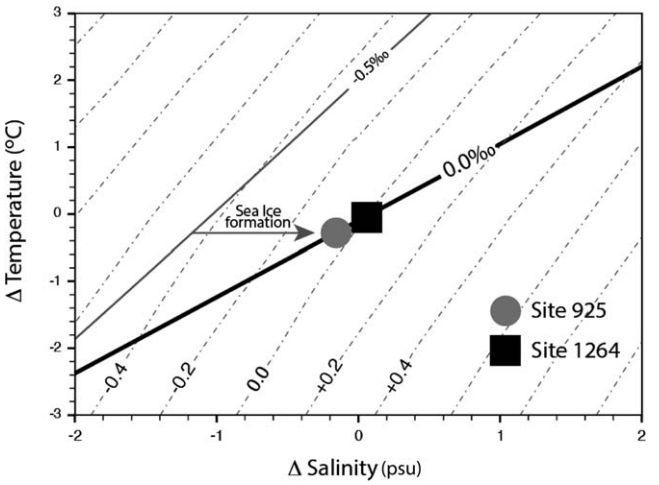

Figure 10. Assessing the implications of large (>0.5‰) Walvis Ridge-North Atlantic δ^{18}O-gradients between ~2.0 and 1.5 Ma. Temperature, salinity, and water mass density anomalies (dashed lines) are shown for the scenario in which source waters for Site 925 have the $\delta^{18}O_{SW}$:salinity relationship of Line 1 in Figure 9 but with the additional imprint of sea ice formation. The figure shows a potential solution for the relative temperature and salinity values of Sites 1264 and 925 assuming a δ^{18}O-gradient of 0.5‰ and minimal density differences. The δ^{18}O isoline (thick black line) for Site 1264 is calculated using the paleotemperature equation from *Kim and O'Neil* [1997] and a $\delta^{18}O_{SW}$:salinity relationship of $\delta^{18}O_{SW} = 0.551 \times S - 19$. Density isolines are calculated for a depth of 2770 m (σ_{2770}).

paleotemperature equation of *Kim and O'Neil* [1997] and a range of possible $\delta^{18}O_{SW}$:salinity relationships, as described below. All calculations are explained in the supporting information. For this exercise, we are not attempting to reconstruct possible absolute temperature and salinity values for Pleistocene conditions at Sites 1264 and 925. Rather, we are seeking to explore the range of temperature and salinity differences needed to minimize density gradients when $\delta^{18}O_b$-gradients are high, under different scenarios of regional $\delta^{18}O_{SW}$:salinity change. By only considering relative $\delta^{18}O_b$ differences, the ice volume effect on $\delta^{18}O_{SW}$ is removed, as this affects all areas of the ocean equally within the mixing time of the ocean (~1–2 kyr). Importantly, the choice of paleotemperature equation does not significantly affect the discussion as the range of the $\delta^{18}O_b$-temperature slope is small between different solutions (~0.21–0.27) [*Zahn and Mix*, 1991] and only relative temperature values are interpreted.

In order to narrow the range of potential explanations of observed δ^{18}O-gradients and to simplify interpretations, we include the following assumptions: (1) source water temperatures must be above the freezing point of seawater, (2) deep waters at Sites 1264 and 925 during times of ~0.5‰ δ^{18}O-gradients are sourced from the high-latitude North Atlantic exclusively, (3) North Atlantic source waters for Sites 1264 and 925 are distinct, (4) density gradients between Sites 1264 and 925, which both lie above the constraining depth of the mid-Atlantic Ridge (MAR), must be minimized, and (5) $\delta^{18}O_{SW}$:salinity changes are modified by inputs from one freshwater and one seawater end-member and/or sea ice formation only.

The first assumption is a physical constraint that must be obeyed. The second assumption is based on the low δ^{13}C-gradients observed between Sites 1264, 925, and other locations within the North Atlantic, which indicate a strong northern signal (Figure 6). The third assumption is based on the large δ^{18}O-gradients observed in Figures 5 and 7. The fourth assumption carries no quantitative constraints but merely seeks to avoid unrealistic ocean dynamics. The fifth assumption is almost certainly not true but is necessary for isolating the impacts of different $\delta^{18}O_{SW}$:salinity scenarios. *Zahn and Mix* [1991] conducted a similar exercise in comparing vertical δ^{18}O-gradients in the North Atlantic and between the North Atlantic and Pacific, during the LGM. For this approach, they considered various deep water $\delta^{18}O_{SW}$:salinity scenarios. The approach taken here differs in this respect as we are assuming an undiluted signal of different NADW components at both locations. Hence, we consider scenarios based on potential $\delta^{18}O_{SW}$:salinity changes originating in North Atlantic source waters.

Figure 8 illustrates a "null-hypothesis" scenario in which source waters for both sites have the same regional $\delta^{18}O_{SW}$:salinity relationship. The modern North Atlantic $\delta^{18}O_{SW}$:salinity values are used here for Site 1264 as a reference throughout this exercise, highlighted by a thicker line. In order to maintain similar densities between Sites 1264 and 925 under this scenario, waters bathing Site 925 would have to be significantly warmer and saltier than those at Site 1264. We consider that temperature and salinity differences of this magnitude ($<\sim\Delta 3.5^{\circ}$C and $<\sim\Delta 1.5$ psu) in the deep ocean, both originating from the North Atlantic region, are highly unlikely. Altering the common $\delta^{18}O_{SW}$:salinity slope does not result in an acceptable solution to this problem. Thus, we conclude that 1264–925 $\delta^{18}O_b$-gradients are at least partially due to local/regional differences in $\delta^{18}O_{SW}$:salinity.

Figure 9 considers scenarios of changing freshwater and seawater end-members. We apply these changes to the source waters of Site 925 only, keeping the Site 1264 as a fixed reference. In the previous section, we suggested that deep waters bathing Site 1264 between ~2.0 and 1.5 Ma were sourced from the southeast Nordic seas, similar to ISOW. In line with the modern situation, it is expected that deep waters in the West Atlantic bathing Site 925 had a stronger influence from higher latitudes, such as Arctic deep waters overflowing as part of Denmark Strait Overflow Water (DSOW), but may have also originated from open ocean convection in the high-latitude North Atlantic, such as Labrador Sea Water (LSW) [*Dickson and Brown*, 1994]. Surface waters in these regions carry a signature of lower $\delta^{18}O_{SW}$ and salinity and are influenced by freshwaters with lower $\delta^{18}O$ values, compared to surface waters entering the southeast Nordic seas [*Frew et al*., 2000; *LeGrande and Schmidt*, 2006]. Accordingly, we adjust the hypothetical $\delta^{18}O_{SW}$:salinity relationship for Site 925 by lowering the freshwater end-member $\delta^{18}O$ value (Line 1) and lowering the seawater end-member $\delta^{18}O$ and salinity values (Lines 2 and 3, respectively). Lowering the freshwater end-member $\delta^{18}O$ value, without altering the seawater end-member, results in a steeper $\delta^{18}O_b$ isoline. Lowering the salinity and $\delta^{18}O$ of the seawater end-member, meanwhile, maintains a parallel $\delta^{18}O_b$ isoline but increases and decreases density differences, respectively. Thus, a combination of lower $\delta^{18}O$ values of freshwater and seawater end-members for deep waters sourcing Site 925 would yield a solution for reducing Site 1264–925 density gradients. A change in $\delta^{18}O_{SW}$ without concomitant changes in salinity within the North Atlantic, however, is an unlikely scenario. Hence, the new position of the $\delta^{18}O_b$ isoline due to lower $\delta^{18}O_{SW}$ values would likely be at least partially offset by lower salinities.

Figure 10 shows the potential influence of sea ice formation on the $\delta^{18}O_b$ signal at Site 925. Taking the scenario of Line 1 in Figure 2, the addition of sea ice formation offers conditions whereby $\delta^{18}O_b$-gradients between Sites 1264–925 could have existed without any differences in water mass temperature and salinity. This is not a unique solution as the additional imprint of sea ice formation to various scenarios can also resolve Site 1264–925 density differences but merely illustrates the potential influence of sea ice formation.

The same arguments presented above for differences between Sites 1264 and 925 may also be made for differences between Sites 1267 and 929. The situation for these deeper sites may, however, permit stronger east-west density differences to exist due to the physical separation of the East and West Atlantic at these depths by the MAR. Indeed, it is probable that ISOW advecting to Sites 1267 and 1264 was a superdense water mass, in order to account for the fact that such high $\delta^{18}O_b$ values are not recorded elsewhere in the Atlantic.

Previous studies investigating possible sources of $\delta^{18}O$ variability in foraminifera have highlighted the importance of considering temporal and spatial changes in $\delta^{18}O_{SW}$:salinity relationships [*Rohling and Bigg*, 1998; *Schmidt*, 1999; *Bauch and Bauch*, 2001; *Wadley et al*., 2002]. A recent study has examined the impact of changes in sea ice formation between glacial and interglacial states on $\delta^{18}O_{SW}$ using an isotope-enabled climate model [*Brennan et al*., 2013]. The results suggested that sea ice formation imprints are negligible for glacial-interglacial $\delta^{18}O$ variability in benthic foraminifera. Only in the surface waters (<400 m) of the Labrador Sea and the northeastern North Atlantic is a small ($<\Delta 0.13‰$) sea ice imprint seen. These results are attributable to dilution of the low $\delta^{18}O_{SW}$ signature from brines by surrounding water masses, and competing $\delta^{18}O_{SW}$ changes in the opposite direction due to factors such as evaporation, precipitation, freshwater runoff, and ocean circulation. This is in line with analogies to modern processes that cause low $\delta^{18}O_{SW}$ anomalies today. *Bauch and Bauch* [2001] evaluated these modern processes in order to explain low $\delta^{18}O_b$ values recorded in the Nordic seas during the last glacial cycle. They argued that only under certain conditions could sea ice formation contribute a sufficient volume of brines that remain relatively undiluted so as to account for ~1‰ lower $\delta^{18}O_b$ values observed in the deep Nordic seas during the LGM. These conditions could have been possible on shallow shelf areas, such as the Barents Sea, but only with extensive volumes of sea ice formation. An alternative and more likely scenario, they suggest, was that low $\delta^{18}O_{SW}$ values resulted from the influence of highly ^{18}O-depleted ($\delta^{18}O$ of $<-40‰$) meltwater, which acted to steepen the $\delta^{18}O_{SW}$:salinity slope (e.g., Line 1 in Figure 9). Such conditions exist during the formation of supercooled deep water beneath floating ice shelves, as is the case in the Weddell Sea today [*Schlosser et al*., 1990; *Weppernig et al*., 1996].

In a separate isotope modeling study, *Wadley et al*. [2002] found that glacial-interglacial changes in North Atlantic $\delta^{18}O_{SW}$ distributions are sensitive to mixing between different surface water masses with distinct $\delta^{18}O_{SW}$ signatures, such as the relative influx of water through the Bering Strait. They also found that the

Arctic was highly depleted in $\delta^{18}O_{SW}$ due to very low $\delta^{18}O$ freshwater Arctic runoff, creating steep $\delta^{18}O_{SW}$:-salinity gradients and influencing North Atlantic surface waters down to ~50°N. Meanwhile, south of ~50°N, surface waters carried a high $\delta^{18}O_{SW}$ signature from lower latitudes and had a low $\delta^{18}O_{SW}$:salinity gradient. Where the North Atlantic Current (NAC) flowed into the Northeast Atlantic, surface water $\delta^{18}O_{SW}$ values increased by over 1‰ in under 10° of latitude, tracking the boundary between polar and subtropical origin waters [*Wadley et al*., 2002].

The emergence of large $\delta^{18}O_b$-gradients at Walvis Ridge sites at ~2.4 Ma is therefore well explained by the influence of lower latitude surface waters, with high salinity and $\delta^{18}O_{SW}$, in the Nordic seas. Enhanced salinity, together with surface water cooling, would have provided conditions for enhanced deep water formation, which was subsequently exported into the East Atlantic with a high $\delta^{18}O_b$ signature. In addition, an increase in supply of MOW to the North Atlantic [*Zahn and Sarnthein*, 1987], or southward flow at depth [*Bickert and Mackensen*, 2003], may have also contributed to higher salinity and $\delta^{18}O_{SW}$ conditions at Walvis Ridge. Comparatively low $\delta^{18}O_b$ values at Sites 925 and 929, meanwhile, could have resulted from deep waters forming at higher latitudes under the influence of extremely low freshwater $\delta^{18}O$ values, such as from surface runoff or melting underneath marine terminating ice sheets. Furthermore, if deep waters formed in shallow shelf regions, then the influence of sea ice formation may have also contributed to low $\delta^{18}O_b$ values.

6. Summary and Conclusions

Comparisons of regional stacks, each containing five to eight records, indicate that average Pacific-North Atlantic $\delta^{18}O_b$-gradients have varied within the range of ~0–0.25‰ during the Plio-Pleistocene. The sign and trend of this gradient is consistent with differences in bottom water Mg/Ca-based temperature reconstructions between the Pacific [*Elderfield et al*., 2012] and North Atlantic [*Sosdian and Rosenthal*, 2009]. However, values were considerably affected by the inclusion of $\delta^{18}O_b$ records from Ceara Rise in the western equatorial North Atlantic. These sites are situated near the core of the modern Deep Western Boundary Current, which currently serves as a main export pathway for NADW. Thus, the comparatively low $\delta^{18}O_b$ values for Ceara Rise sites imply unique temperature and/or $\delta^{18}O_{SW}$ properties for a key component of NADW.

Through comparisons with new records from Sites 1264 and 1267, unique water mass $\delta^{18}O_b$ properties have also been identified in the Southeast Atlantic, on the northern flank of Walvis Ridge. These properties become most prominent during the early to mid-Pleistocene (~2.4–1.3 Ma), when $\delta^{18}O_b$-gradients with records from Ceara Rise average ~0.5‰, and maximum gradient values reach up to ~1‰. Bathymetric constraints and $\delta^{18}O_b$-gradients between records from surrounding sites imply that deep waters bathing the northern flank of Walvis Ridge have been predominantly northern sourced throughout the Plio-Pleistocene, in agreement with comparisons of $\delta^{13}C$ records. Therefore, we propose the existence of a new water mass, with $\delta^{18}O_b$ values distinctly higher than values widely recorded in the North Atlantic. These features indicate a possible source as being dense, ^{18}O-enriched overflow waters from the Nordic seas. The export pathway of this water mass is inferred to be along the abyssal Eastern Atlantic, a region for which benthic stable isotope records have not yet been established. Such a scenario represents nonanalogue conditions in Atlantic Meridional Overturning Circulation and places emphasis on the importance of the Nordic seas in influencing climate. It is also possible that MOW contributed to the high $\delta^{18}O_b$ signal at Walvis Ridge via increased contribution to deep water formation in the North Atlantic, or southward flow at depth.

The observed $\delta^{18}O_b$-gradients were investigated using temperature-salinity plots with calculated density and $\delta^{18}O_b$ isolines. A range of local/regional $\delta^{18}O_{SW}$:salinity relationships were explored in order to explain large (0.5‰) $\delta^{18}O_b$-gradients between Sites 1264 and 925, which lie at comparable depths in the East and West Atlantic, respectively. The results indicate that the $\delta^{18}O_b$-gradients cannot be satisfactorily explained by temperature and salinity differences alone. Hence, distinct $\delta^{18}O_{SW}$:salinity relationships appear to be required for sources waters that bathe Sites 1264 and 1267, compared to those filling much of the Northwest Atlantic. We suggest that the high $\delta^{18}O_b$ values recorded at Sites 1264 and 1267 are well explained if source waters are under the influence of a low-latitude surface water signal, while lower $\delta^{18}O_b$ values recorded in the Northwest Atlantic are likely the result of a high-latitude source water signal.

The implications of our results are thus threefold. First, $\delta^{18}O_b$ records may be instrumental in diagnosing different water masses and constraining deep water circulation during the Plio-Pleistocene. Second,

interpretations of $\delta^{18}O_{SW}$ changes from $\delta^{18}O_b$ records, particularly from the Atlantic, should consider the potential for changes in the source water $\delta^{18}O_{SW}$:salinity relationship through time. Finally, the inferred connection between low-latitude surface waters and deep water export into the abyssal East Atlantic suggests a role for Atlantic Meridional Overturning Circulation in shaping Plio-Pleistocene climate change through enhanced oceanic northward heat transport.

Acknowledgments
The data for this paper will be available online at http://www.ncdc.noaa.gov/data-access/paleoclimatology-data. This work was supported by a NERC Ph.D. studentship to D. Bell. Colin Chilcott is thanked for assistance with the mass spectrometer. This manuscript was improved substantially as a result of reviews from three anonymous reviewers, to whom we are grateful.

References

Adkins, J. F., K. McIntyre, and D. P. Schrag (2002), The salinity, temperature, and δ18O of the glacial deep ocean, *Science*, *298*(5599), 1769–1773, doi:10.1126/science.1076252.

Andersson, C., D. A. Warnke, J. E. T. Channell, J. Stoner, and E. Jansen (2002), The mid-Pliocene (4.3–2.6 Ma) benthic stable isotope record of the Southern Ocean: ODP Sites 1092 and 704, Meteor Rise, *Palaeogeogr. Palaeoclimatol. Palaeoecol.*, *182*, 165–181.

Arhan, M., H. Mercier, and Y.-H. Park (2003), On the deep water circulation of the eastern South Atlantic Ocean, *Deep Sea Res., Part I*, *50*(7), 889–916, doi:10.1016/S0967-0637(03)00072-4.

Bauch, D., and H. A. Bauch (2001), Last glacial benthic foraminiferal δ180 anomalies in the polar North Atlantic: A modern analogue evaluation, *J. Geophys. Res.*, *106*(C5), 9135–9143.

Bickert, T., and A. Mackensen (2003), Last Glacial to Holocene changes in South Atlantic deep water circulation, in *The South Atlantic in the Late Quaternary: Reconstruction of Material Budgets and Current Systems*, edited by G. Wefer, S. Mulitza, and V. Ratmeyer, pp. 671–693, Springer, Berlin.

Bickert, T., W. Curry, and G. Wefer (1997), Late Pliocene to Holocene (2.6–0 Ma) western equatorial Atlantic deep-water circulation: Inferences from benthic stable isotopes, in *Proc. Ocean Drill. Program Sci. Results*, vol. 154, Ocean Drill. Program, College Station, Tex.

Billups, K., A. C. Ravelo, and J. C. Zachos (1997), 21. Early Pliocene deep-water circulation: Stable isotope evidence for enhanced Northern Component Deep Water, *Proc. Ocean Drill. Program Sci. Results*, *154*, 319–330.

Billups, K., A. Ravelo, and J. C. Zachos (1998), Early Pliocene deep water circulation in the western equatorial Atlantic: Implications for high-latitude climate change, *Paleoceanography*, *13*(1), 84–95.

Bintanja, R., and R. S. W. van de Wal (2008), North American ice-sheet dynamics and the onset of 100,000-year glacial cycles. *Nature*, *454*(7206), 869–872, doi:10.1038/nature07158.

Brennan, C. E., K. J. Meissner, M. Eby, C. Hillaire-Marcel, and A. J. Weaver (2013), Impact of sea ice variability on the oxygen isotope content of seawater under glacial and interglacial conditions, *Paleoceanography*, *28*, 388–400, doi:10.1002/palo.20036.

Candela, J. (2001), Mediterranean water and global circulation, in *Ocean Circulation and Climate—Observing and Modelling the Global Ocean: International Geophysics Series*, edited by G. Siedler, J. Church, and J. Gould, 715 pp., Academic, San Diego, Calif.

Connary, S. D., and M. Ewing (1974), Penetration of Antarctic bottom water from the Cape Basin into the Angola Basin, *J. Geophys. Res.*, *79*(3), 463–469.

Craig, H., and L. Gordon (1965), Deuterium and oxygen-18 variations in the ocean and the marine atmosphere, in *Stable Isotopes on Oceanographic Studies and Paleotemperatures*, edited by E. Tongiori, pp. 9–130, Natl. Res. Counc., Pisa, Italy.

Cutler, K., R. Edwards, F. Taylor, H. Cheng, J. Adkins, C. Gallup, P. Cutler, G. Burr, and A. Bloom (2003), Rapid sea-level fall and deep-ocean temperature change since the last interglacial period, *Earth Planet. Sci. Lett.*, *206*(3–4), 253–271, doi:10.1016/S0012-821X(02)01107-X.

de Boer, B., R. S. W. van de Wal, L. J. Lourens, and R. Bintanja (2012), Transient nature of the Earth's climate and the implications for the interpretation of benthic records, *Palaeogeogr. Palaeoclimatol. Palaeoecol.*, *335–336*, 4–11, doi:10.1016/j.palaeo.2011.02.001.

Dickson, R. R., and J. Brown (1994), The production of North Atlantic Deep Water: Sources, rates and pathways, *J. Geophys. Res.*, *99*(C6), 12,319–12,341.

Duplessy, J.-C., N. J. Shackleton, R. G. Fairbanks, L. Labeyrie, D. W. Oppo, and N. Kallel (1988), Deepwater source variations during the last climatic cycle and their impact on global deepwater circulation, *Paleoceanography*, *3*(3), 343–360.

Duplessy, J.-C., L. Labeyrie, and C. Waelbroeck (2002), Constraints on the ocean oxygen isotopic enrichment between the Last Glacial Maximum and the Holocene: Paleoceanographic implications, *Quat. Sci. Rev.*, *21*(1–3), 315–330, doi:10.1016/S0277-3791(01)00107-X.

Edgar, K. M., H. Pälike, and P. A. Wilson (2013), Testing the impact of diagenesis on the δ 18 O and δ 13 C of benthic foraminiferal calcite from a sediment burial depth transect in the equatorial Pacific, *Paleoceanography*, *28*, 468–480, doi:10.1002/palo.20045.

Elderfield, H., P. Ferretti, M. Greaves, S. Crowhurst, I. N. McCave, D. A. Hodell, and A. M. Piotrowski (2012), Evolution of ocean temperature and ice volume through the mid-Pleistocene climate transition, *Science*, *337*(August), 704–709, doi:10.1594/PANGAEA.786205.

Emiliani, C. (1955), Pleistocene temperatures, *J. Geol.*, *63*, 538–578.

Feldmeijer, W., B. Metcalfe, P. Scussolini, and K. Arthur (2013), The effect of chemical pretreatment of sediment upon foraminiferal-based proxies, *Geochem. Geophys. Geosyst.*, *14*, 3996–4014, doi:10.1002/ggge.20233.

Fleischmann, U., H. Hildebrandt, A. Putzka, and R. Bayer (2001), Transport of newly ventilated deep water from the Iceland Basin to the Westeuropean Basin, *Deep Sea Res., Part I*, *48*(8), 1793–1819, doi:10.1016/S0967-0637(00)00107-2.

Flower, B. P., D. W. Oppo, J. F. Mcmanus, K. A. Venz, D. A. Hodell, and J. L. Cullen (2000), North Atlantic intermediate to deep water circulation and chemical stratification during the past 1 Myr, *Paleoceanography*, *15*(4), 388–403.

Frew, R. D., P. F. Dennis, K. J. Heywood, M. P. Meredith, and S. M. Boswell (2000), The oxygen isotope composition of water masses in the northern North Atlantic, *Deep Sea Res., Part I*, *47*(12), 2265–2286, doi:10.1016/S0967-0637(00)00023-6.

Hall, I., I. McCave, and N. Shackleton (2001), Intensified deep Pacific inflow and ventilation in Pleistocene glacial times, *Nature*, *412*, 809–812.

Hansen, B., and S. Østerhus (2000), North Atlantic–Nordic seas exchanges, *Prog. Oceanogr.*, *45*(2), 109–208, doi:10.1016/S0079-6611(99)00052-X.

Harris, S. E. (2002), Data report: Late Pliocene-Pleistocene carbon and oxygen stable isotopes from benthic foraminiferas at Ocean Drilling Program Site 1123 in the southwest Pacific, in *Proc. Ocean Drill. Program Sci. Results*, vol. 181, Ocean Drill. Program, College Station, Tex.

Herbert, T. D. (2001), Collapse of the California current during glacial maxima linked to climate change on land, *Science*, *293*(5527), 71–76, doi:10.1126/science.1059209.

Hodell, D. A., and K. A. Venz (1992), Toward a high-resolution stable isotopic record of the Southern Ocean during the Pliocene-Pleistocene (4.8 to 0.8 Ma), *Antarct. Res. Ser.*, *56*, 265–310.

Hodell, D. A., and K. A. Venz-curtis (2006), Late Neogene history of deepwater ventilation in the Southern Ocean, *Geochem. Geophys. Geosyst.*, *7*(9), Q09001, doi:10.1029/2005GC001211.

Hogg, N., and A. Thurnherr (2005), A zonal pathway for NADW in the South Atlantic, *J. Oceanogr.*, *61*(1991), 493–507.

Imbrie, J. et al. (1992), On the structure and origin of major glaciation cycles 1. Linear responses to Milankovitch forcing, *Paleoceanography*, *7*(6), 701–738.
Kim, S. T., and J. R. O'Neil (1997), Equilibrium and nonequilibrium oxygen isotope effects in synthetic carbonates, *Geochim. Cosmochim. Acta*, *61*(16), 3461–3475.
LeGrande, A. N., and G. A. Schmidt (2006), Global gridded data set of the oxygen isotopic composition in seawater, *Geophys. Res. Lett.*, *33*, L12604, doi:10.1029/2006GL026011.
Leonard, G. H., P. J. Langhorne, M. J. M. Williams, R. Vennell, C. R. Purdie, D. E. Dempsey, T. G. Haskell, and R. D. Frew (2011), Evolution of supercooling under coastal Antarctic sea ice during winter, *Antarct. Sci.*, *23*(04), 399–409, doi:10.1017/S0954102011000265.
Lisiecki, L. E., and M. E. Raymo (2005), A Pliocene-Pleistocene stack of 57 globally distributed benthic δ18O records, *Paleoceanography*, *20*, PA1003, doi:10.1029/2004PA001071.
Lisiecki, L. E., and M. E. Raymo (2009), Diachronous benthic δ18O responses during late Pleistocene terminations, *Paleoceanography*, *24*, PA3210, doi:10.1029/2009PA001732.
Lozier, M., W. Owens, and R. Curry (1995), The climatology of the North Atlantic, *Prog. Oceanogr.*, *36*, 1–44.
Martin, P. A., D. W. Lea, Y. Rosenthal, N. J. Shackleton, M. Sarnthein, and T. Papenfuss (2002), Quaternary deep sea temperature histories derived from benthic foraminiferal Mg/Ca, *Earth Planet. Sci. Lett.*, *198*(1–2), 193–209, doi:10.1016/S0012-821X(02)00472-7.
McIntyre, K., A. C. Ravelo, and M. L. Delaney (1999), North Atlantic Intermediate Waters in the late Pliocene to early Pleistocene, *Paleoceanography*, *14*(3), 324–335.
McManus, J. F. (1999), A 0.5-million-year record of millennial-scale climate variability in the North Atlantic, *Science*, *283*(5404), 971–975, doi:10.1126/science.283.5404.971.
Meland, M. Y., T. M. Dokken, E. Jansen, and K. Hevrøy (2008), Water mass properties and exchange between the Nordic seas and the northern North Atlantic during the period 23-6 ka: Benthic oxygen isotopic evidence, *Paleoceanography*, *23*, PA1210, doi:10.1029/2007PA001416.
Meyers, S. R., and L. A. Hinnov (2010), Northern Hemisphere glaciation and the evolution of Plio-Pleistocene climate noise, *Paleoceanography*, *25*, PA3207, doi:10.1029/2009PA001834.
Mix, A. C., N. G. Pisias, W. Rugh, J. Wilson, A. Morey, and T. K. Hagelberg (1995a), 17. Benthic foraminifer stable isotope record from Site 849 (0–5 Ma): Local and global climate changes, *Proc. Ocean Drill. Program Sci. Results*, *138*, 371–412.
Mix, A. C., J. Le, and N. J. Shackleton (1995b), 43. Benthic foraminiferal stable isotope stratigraphy of Site 846: 0–1.8 Ma, *Proc. Ocean Drill. Program Sci. Results*, *138*, 839–854.
Mudelsee, M., and M. E. Raymo (2005), Slow dynamics of the Northern Hemisphere glaciation, *Paleoceanography*, *20*, PA4022, doi:10.1029/2005PA001153.
Oppo, D. W., J. F. McManus, and J. L. Cullen (1998), Abrupt climate events 500,000 to 340,000 years ago: Evidence from subpolar North Atlantic sediments, *Science*, *279*(5355), 1335–1338, doi:10.1126/science.279.5355.1335.
Ostermann, D. R., and W. B. Curry (2000), Calibration of stable isotopic data: An enriched δ180 standard used for source gas mixing detection and correction, *Paleoceanography*, *15*(3), 353–360.
Paillard, D., L. Labeyrie, and P. Yiou (1996), Macintosh Program performs time-series analysis, *Eos, Trans. AGU*, *77*(39), 379, doi:10.1029/96EO00259.
Rathmann, S., and H. Kuhnert (2008), Carbonate ion effect on Mg/Ca, Sr/Ca and stable isotopes on the benthic foraminifera Oridorsalis umbonatus off Namibia, *Mar. Micropaleontol.*, *66*(2), 120–133, doi:10.1016/j.marmicro.2007.08.001.
Raymo, M., W. F. Ruddiman, J. Backman, B. M. Clement, and D. G. Martinson (1989), Late Pliocene variation in Northern Hemisphere ice sheets and North Atlantic Deep Water circulation, *Paleoceanography*, *4*(4), 413–446.
Raymo, M. E. (1997), The timing of major climate terminations, *Paleoceanography*, *12*(4), 577–585.
Raymo, M. E., D. A. Hodell, and E. Jansen (1992), Response of deep ocean circulation to initiation of Northern Hemisphere glaciation (3–2 Ma), *Paleoceanography*, *7*(5), 645–672.
Raymo, M. E., D. W. Oppo, B. P. Flower, D. A. Hodell, J. F. McManus, K. A. Venz, H. F. Kleiven, and K. McIntyre (2004), Stability of North Atlantic water masses in face of pronounced climate variability during the Pleistocene, *Paleoceanography*, *19*, PA2008, doi:10.1029/2003PA000921.
Reid, J. L. (1994), On the total geostrophic circulation of the North Atlantic Ocean: Flow patterns, tracers, and transports, *Prog. Oceanogr.*, *33*(1), 1–92, doi:10.1016/0079-6611(94)90014-0.
Rohling, E. J., and G. R. Bigg (1998), Paleosalinity and δ18O: A critical assessment, *J. Geophys. Res.*, *103*(C1), 1307–1318.
Ruddiman, W. F., M. E. Raymo, D. G. Martinson, S. C. Clemens, and J. Backman (1989), Mid-Pleistocene evolution of Northern Hemisphere climate, *Paleoceanography*, *4*, 353–414.
Sarnthein, M., K. Winn, S. J. A. Jung, J. Duplessy, L. Labeyrie, H. Erlenkeuser, and G. Ganssen (1994), Changes in East Atlantic deepwater circulation over the last 30,000 years: Eight time slice reconstructions, *Paleoceanography*, *9*(2), 209–267.
Schlosser, P., R. Bayer, A. Foldvik, T. Gammelsrød, G. Rohardt, and K. O. Münnich (1990), Oxygen 18 and helium as tracers of ice shelf water and water/ice interaction in the Weddell Sea, *J. Geophys. Res. Ocean.*, *95*(C3), 3253–3263.
Schmidt, G. A. (1999), Forward modeling of carbonate proxy data from planktonic foraminifera using oxygen isotope tracers in a global ocean model, *Paleoceanography*, *14*(4), 482–497, doi:10.1029/1999PA900025.
Schmiedl, G., A. Mackensen, and P. J. Miiller (1997), Recent benthic foraminifera from the eastern South Atlantic Ocean: Dependence on food supply and water masses, *Mar. Micropaleontol.*, *32*(97), 249–287.
Schrag, D., G. Hampt, and D. Murray (1996), Pore fluid constraints on the temperature and oxygen isotopic composition of the glacial ocean, *Science*, *272*(5270), 1930–1932.
Shackleton, N. (1967), Oxygen isotope analyses and Pleistocene temperatures re-assessed, *Nature*, *215*, 15–17.
Shackleton, N. (2000), The 100,000-year ice-age cycle identified and found to lag temperature, carbon dioxide, and orbital eccentricity, *Science*, *289*(5486), 1897–902.
Shackleton, N. J., and M. A. Hall (1984), Chapter 16. Oxygen and carbon isotope stratigraphy of Deep Sea Drilling Project hole 552a: Plio-Pleistocene glacial history, *Initial Rep. Deep Sea Drill. Proj.*, *81*, 599–609.
Shackleton, N. J., and N. D. Opdyke (1973), Oxygen isotope and Palaeomagnetic stratigraphy of equatorial Pacific core V28–238: Oxygen isotope temperatures and ice volumes on a 10^5 year and 10^6 year scale, *Quat. Res.*, *3*, 39–55.
Shackleton, N. J., A. Bergerm, and W. R. Peltier (1990), An alternative astronomical calibration of the lower Pleistocene timescale based on ODP site 677, *Trans. R. Soc. Edinburgh Earth Sci.*, *81*, 251–261.
Shackleton, N. J., M. A. Hall, and D. Pate (1995), 15. Pliocene stable isotope stratigraphy of site 846, *Proc. Ocean Drill. Program Sci. Results*, *138*, 337–355.

Siddall, M., B. Hönisch, C. Waelbroeck, and P. Huybers (2010), Changes in deep Pacific temperature during the Mid-Pleistocene Transition and quaternary, *Quat. Sci. Rev.*, *29*(1–2), 170–181, doi:10.1016/j.quascirev.2009.05.011.

Skinner, L. C., and N. J. Shackleton (2005), An Atlantic lead over Pacific deep-water change across Termination I: Implications for the application of the Marine Isotope Stage stratigraphy, *Quat. Sci. Rev.*, *24*(5–6), 571–580, doi:10.1016/j.quascirev.2004.11.008.

Smethie, W. M., R. A. Fine, A. Putzka, and E. Peter (2000), Tracing the flow of North Atlantic Deep Water using chlorofluorocarbons, *J. Geophys. Res.*, *105*, 14,297–14,323.

Sosdian, S., and Y. Rosenthal (2009), Deep-sea temperature and ice volume changes across the Pliocene-Pleistocene climate transitions, *Science*, *325*, 306–310.

Sosdian, S., and Y. Rosenthal (2010), Response to comment on "Deep-sea temperature and ice volume changes across the Pliocene-Pleistocene climate transitions," *Science*, *328*(5985), 1480–1480, doi:10.1126/science.1186768.

Spero, H., J. Bijma, D. Lea, and B. Bemis (1997), Effect of seawater carbonate concentration on foraminiferal carbon and oxygen isotopes, *Nature*, *390*, 497–500.

Stramma, L., and M. England (1999), On the water masses and mean circulation of the South Atlantic Ocean, *J. Geophys. Res.*, *104*(C9), 20,863–20,883.

Tian, J., P. Wang, X. Cheng, and Q. Li (2002), Astronomically tuned Plio-Pleistocene benthic δ18O record from South China Sea and Atlantic-Pacific comparison, *Earth Planet. Sci. Lett.*, *203*, 1015–1029.

Tiedemann, R., and S. O. Franz (1997), 20. Deep-water circulation, chemistry, and terrigenous sediment supply in the equatorial Atlantic during the Pliocene, 3.3–2.6 Ma and 5–4.5 Ma, *Proc. Ocean Drill. Program Sci. Results*, *154*, 299–318.

Tiedemann, R., M. Sarnthein, and N. J. Shackleton (1994), Astronomical timescale for the Pliocene Atlantic d18O and dust flux records of Ocean Drilling Program site 659, *Paleoceanography*, *9*(4), 619–638.

Tiedemann, R., A. Sturm, S. Steph, S. P. Lund, and J. S. Stoner (2007), 4. Astronomically calibrated timescales from 6 to 2.5 Ma and benthic isotope stratigraphies, sites 1236, 1237, 1239 and 1241, *Proc. Ocean Drill. Program Sci. Results*, *202*, 1–69, doi:10.2973/odp.proc.sr.202.210.2007.

Venti, N. L., and K. Billups (2012), Stable-isotope stratigraphy of the Pliocene–Pleistocene climate transition in the northwestern subtropical Pacific, *Palaeogeogr. Palaeoclimatol. Palaeoecol.*, *326–328*, 54–65, doi:10.1016/j.palaeo.2012.02.001.

Venz, K. A., and D. A. Hodell (2002), New evidence for changes in Plio-Pleistocene deep water circulation from Southern Ocean ODP Leg 177 Site 1090, *Paleoceanogr. Palaeoclimatol. Palaeoecol.*, *182*, 197–220.

Wadley, M. R., G. R. Bigg, E. J. Rohling, and A. J. Payne (2002), On modelling present-day and last glacial maximum oceanic δ18O distributions, *Global Planet. Change*, *32*, 89–109.

Waelbroeck, C., L. Labeyrie, E. Michel, J. C. Duplessy, J. F. McManus, K. Lambeck, E. Balbon, and M. Labracherie (2002), Sea-level and deep water temperature changes derived from benthic foraminifera isotopic records, *Quat. Sci. Rev.*, *21*(1–3), 295–305, doi:10.1016/S0277-3791(01)00101-9.

Waelbroeck, C., L. C. Skinner, L. Labeyrie, J.-C. Duplessy, E. Michel, N. Vazquez Riveiros, J.-M. Gherardi, and F. Dewilde (2011), The timing of deglacial circulation changes in the Atlantic, *Paleoceanography*, *26*, PA3213, doi:10.1029/2010PA002007.

Weiss, R. F., H. G. Östlund, and H. Craig (1979), Geochemical studies of the Weddell sea, *Deep Sea Res., Part A.*, *26*(10), 1093–1120, doi:http://dx.doi.org/10.1016/0198-0149(79)90059-1.

Weppernig, R., P. Schlosser, S. Khatiwala, and R. G. Fairbanks (1996), Isotope data from Ice Station Weddell: Implications for deep water formation in the Weddell Sea, *J. Geophys. Res.*, *101*(C10), 25,723–25,739.

Yu, J., and W. S. Broecker (2010), Comment on "Deep-sea temperature and ice volume changes across the Pliocene-Pleistocene climate transitions," *Science*, *328*(5985), 1480; author reply 1480, doi:10.1126/science.1186544.

Zachos, J. C., D. Kroon, P. Blum, et al. (2004), Shipboard Scientific Party, Leg 208 summary, in *Proc. Ocean Drill. Program Initial Rep.*, vol. 208, 1–112, Ocean Drilling Program, College Station, Tex.

Zahn, R., and A. C. Mix (1991), Benthic Foraminiferal δ18O in the ocean's temperature-salinity-density field: Constraints on ice age thermohaline circulation, *Paleoceanography*, *6*(1), 1–20.

Zahn, R., and M. Sarnthein (1987), Benthic isotope evidence for changes of the Mediterranean Outflow during the late quaternary, *Paleoceanography*, *2*(6), 543–559.